Ocean Engineering 72 (2013) 287–296

Contents lists available at ScienceDirect

Ocean Engineering

journal homepage: www.elsevier.com/locate/oceaneng

Time domain method for the prediction of pressure fluctuation induced by propeller sheet cavitation: Numerical simulations and experimental validation

Hanshin Seol *

Maritime and Ocean Engineering Research Institute (MOERI)/KIOST, 171 Jang-Dong Yuseong, Daejeon 305-343, Republic of Korea

ARTICLE INFO

Article history:
Received 21 December 2012
Accepted 28 June 2013
Available online 3 August 2013

Keywords:
Pressure fluctuation
Marine propeller
Sheet cavitation
Cavitation tunnel

ABSTRACT

This paper addresses the pressure fluctuation induced by a propeller sheet cavitation. This study applies the acoustic theory proposed by Ffowcs Williams and Hawkings to the prediction of the pressure fluctuation caused by the volume variations of the propeller cavitation. There are two objectives of this study. The first objective is to clarify and analyze the mechanism of the pressure fluctuation induced by the propeller sheet cavitation. The second objective is the evaluation of the developed numerical prediction method. Various factors that affect the pressure fluctuation are numerically simulated and analyzed based on the developed governing equation. The developed time domain prediction method is combined with the vortex lattice method, which solves for the unsteady sheet cavitation on the propeller blades. The numerical prediction results of the newly developed method are compared with the results of a potential-based numerical prediction method and the experimental results from the MOERI medium size cavitation tunnel tests for various operation conditions and propellers. As a result of this study, the pressure fluctuation induced by a propeller sheet cavitation is not simply proportional to the second derivative of the cavitation volume variation and inversely proportional to the distance. The fluctuation is represented by the combined result of the far-field term and the near-field term. Furthermore, various simulation results show that an elaborate prediction requires the overall consideration of the near-field term, the effect of the relative motion of the sources and the retarded time for the measurement position. The developed time domain prediction method provides reasonable results, and these results are in good agreement with the experimental results. In some cases, this method will provide much better results than the potential-based prediction method, especially for the prediction of the location where the maximum amplitude blade rate and the pressure amplitude of higher harmonics.

1. Introduction

Recently, loads on propellers have been increasing due to the need for large and high-speed ships. Therefore, propeller cavitation is increasing, and the resulting adverse effects are becoming an important issue. Cavitation on a propeller induces pressure fluctuations on the hull. The limitation of tip clearance and an increase in higher order pressure fluctuation can cause severe ship vibration and a noise problem. Therefore, a technique allowing for the prediction and control of pressure fluctuations induced by propeller cavitation is needed at the design stage.

The factors causing pressure fluctuation induced by a propeller are classified into three primary parts: changes in the blade loading, rotation of the blade thickness, and the volume change of the propeller cavitation (Carlton, 2007). However, pressure fluctuation due to changes in blade loading and blade thickness are very small compared with the pressure fluctuations caused by cavitation. Various types of propeller cavitation, such as sheet cavitation, tip vortex cavitation, and bubble cavitation, affect the hull pressure fluctuation. The peak pressure fluctuation is measured in a discrete form at the blade rate frequency and is caused by unsteady sheet cavitation (Carlton, 2007).

There have been numerous studies of the pressure fluctuation caused by propeller cavitation (Kinns and Bloor, 2004; Merz et al., 2009; Lee et al., 1992; Cavitation Committee Report, 1987; The Specialist Committee on Cavitation Induced Pressures, 2002).

In recent years numerical prediction method using CFD is introduced and it shows good results (Pereira et al., 2004; Ji et al., 2011, 2012; Kehr and Kao, 2011; Luo et al., 2012; Seo et al., 2008).

* Fax: +82 42 866 3468.
E-mail address: seol@kiost.ac

0029-8018
http://dx.doi.org/10.1016/j.oceaneng.2013.06.030

Most studies investigated the correlation between predictions, model test results, and real ship measurements (Kim et al., 1996). Recently, the potential-based numerical prediction methods have been introduced that consider the physical propeller configuration and operating conditions. However, these numerical prediction methods make it difficult to intuitively understand the governing equation because they are presented in a form that is a result of solving potential-based boundary value problems. Moreover, these equations cannot represent the relative motion of the sources and the retarded time for the measurement point.

This study is designed to find the physical significance of propeller cavitation and pressure fluctuation using a numerical approach based on theory and experimental validation.

To predict the pressure fluctuation induced by propeller sheet cavitation, a modern acoustic methodology is applied. The pressure fluctuation induced by propeller cavitation is generally known to be proportional to the second time derivative of the cavitation volume variation and inversely proportional to the distance from the sources, as shown in Eq. (1) (Blake, 1996).

$$p'(r,t) = \frac{\rho_0 \ddot{Q}(t-r/c)}{4\pi r} = \frac{\rho_0 (R^2\ddot{R} + 2R\dot{R}^2)}{r} \quad (1)$$

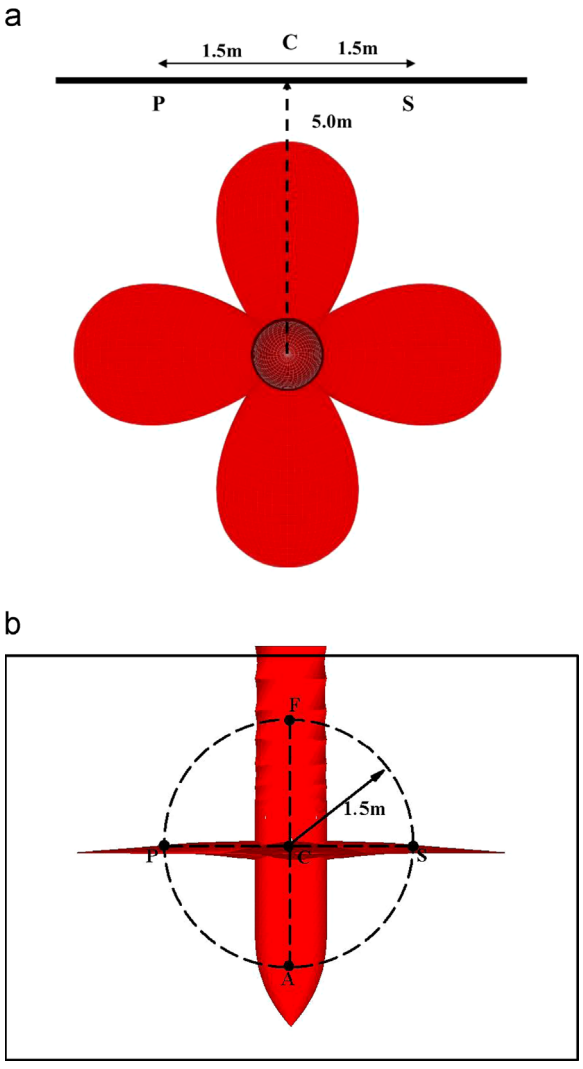

Fig. 1. Simulation model propeller and the location of the computation position; (a) view from the stern, (b) view from the upper side.

However, Eq. (1) is only valid where the pressure fluctuation sources are stationary and the observer is far away from the sources ($r \gg R$). Moreover, the distance between the rotating propeller and the hull is smaller than the length of the pressure waves induced by the propeller sheet cavitation. Pressure fluctuation can be affected by the sheet cavitation motion and the near-field effect. Therefore, Eq. (1) cannot be applied. Nevertheless, it is difficult to find studies in the literature that discuss these problems (Bark, 1988).

Therefore, this study applies the combined hydrodynamic and hydroacoustic method to the prediction of the pressure fluctuation caused by a volume variation in the propeller sheet cavitation,

Table 1
Propeller data and operating condition.

Diameter	6.0 m
Hub-diameter ratio	0.17
Number of blades	4
Propeller rotational speed	120 rpm
Tip clearance	2.0 m
Ship speed (V_S)	15 knots (7.7 m/s)

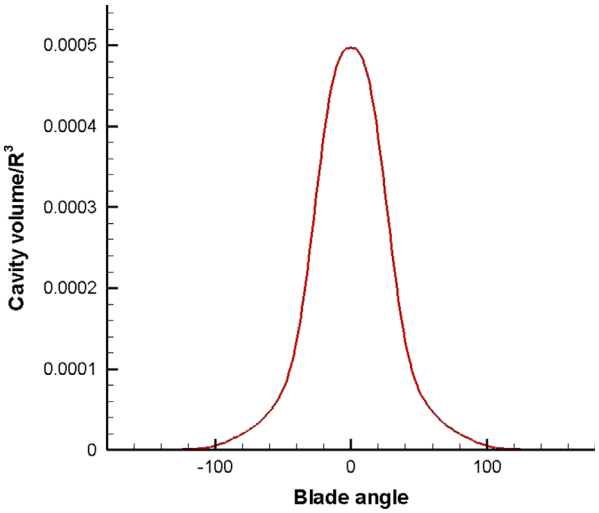

Fig. 2. Numerically simulated volume variation of the sheet cavitation.

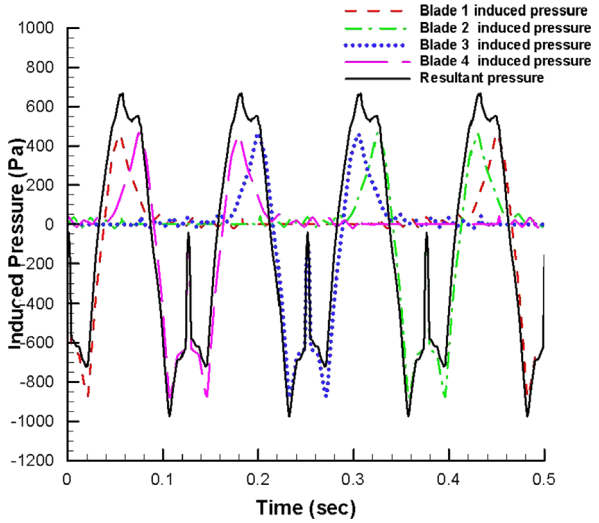

Fig. 3. Induced pressure fluctuation and the resultant pressure time signal at point '*C*.

which has a dominant effect on pressure fluctuation. Theoretical and numerical approaches considering the source motion and the near-field effect due to the rotation of the sheet cavitation are attempted. The findings will improve studies on hull pressure fluctuation in the future.

The paper is organized as follows. Section 2 presents the time domain method for the prediction of the pressure fluctuation and its numerical simulations. Section 3 describes the pressure fluctuation experiments that were performed in the MOERI cavitation tunnel and presents a comparison of the results of the experimental data and the newly developed time domain prediction results.

2. Time domain method for the prediction of pressure fluctuation

2.1. Flow analysis and time domain prediction method

Potential based vortex lattice method is coupled with acoustic analogy method for the prediction of pressure fluctuation.

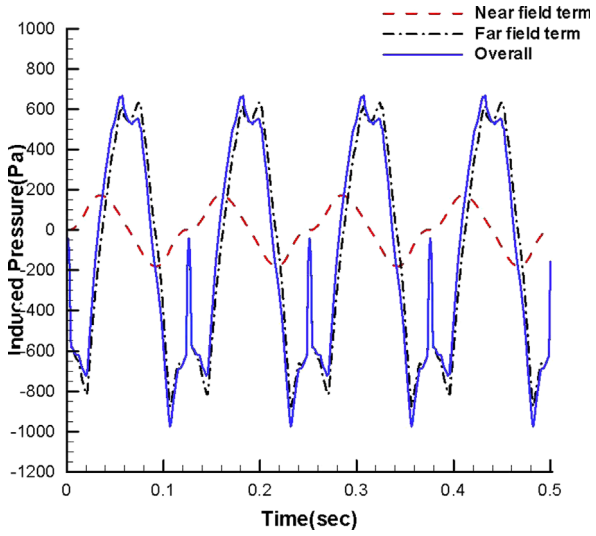

Fig. 4. Induced pressure fluctuation and the resultant pressure time signal at point '*C*' (near-field term & far-field term).

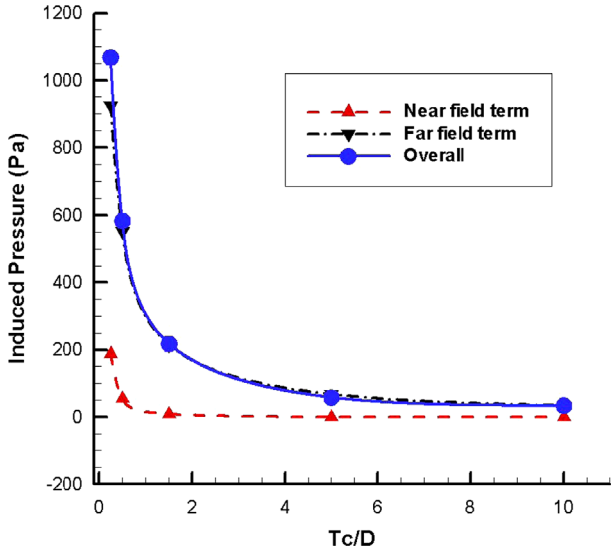

Fig. 5. Pressure fluctuation according to the tip clearance (near-field term and far-field term).

The vortex lattice method performs analysis of propeller performance and cavitation volume variation. In the vortex lattice approach the continuous distributions of vortices and sources are replaced by a finite set of straight line elements of constant strength whose end points lie on the blade camber surface. (Carlton, 2007) A potential based lifting surface methods and their application to propeller technology began in the 1980s. A lifting surface method for marine propeller was developed by Kerwin and Lee (1987) at the Massachussetts Institute of Technology. The fundamentals and details of lifting surface method are well described in works of Lee (1979, 1992) and Kinnas and Fine (1992).

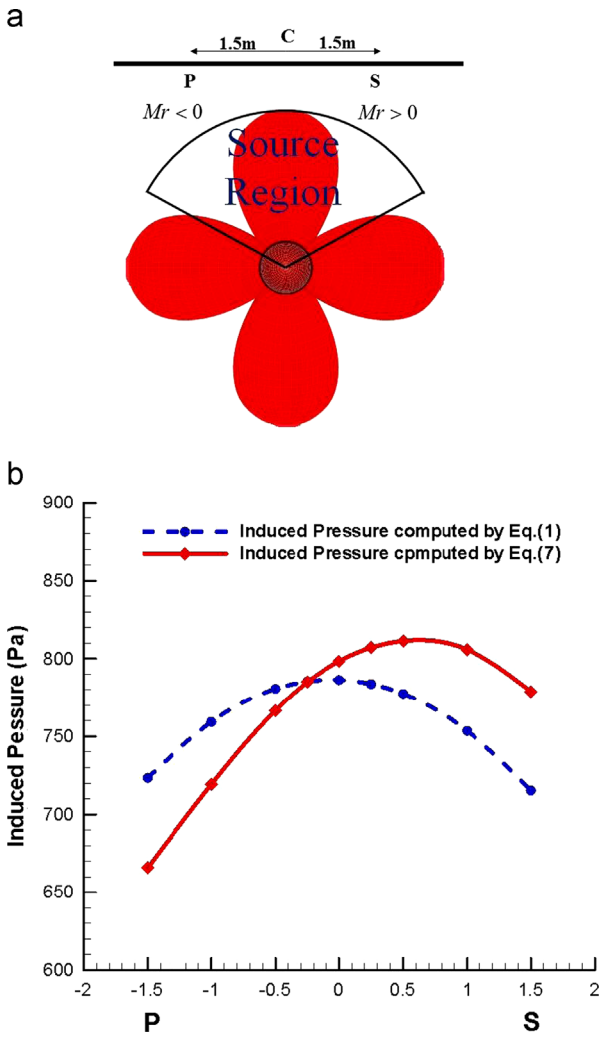

Fig. 6. Induced pressure fluctuation (effect of the source movement); (a) Schematic diagram (b) Induced pressure fluctuation from point '*P*' to point '*S*'.

Table 2
Principal particulars of propellers.

Propeller	Propeller A	Propeller B	Propeller C
Diameter	5.2 m	5.2 m	4.6 m
Hub-diameter ratio	0.17	0.2	0.16
Number of blades	4	4	5
Effective skew	19°	23°	28.5°
Expanded area	1.686 m	1.630 m	1.2512 m
$(P/D)_{mean}$	0.705	0.681	0.867

Potential based flow analysis and pressure fluctuation prediction method are widely used in propeller design. These numerical methods are developed in MOERI in 1990′s.

The calculation method is quasi-stationary. The pressure distribution on the blade surface and sheet cavitation volume is computed at every 6° per time step.

Pressure fluctuation induced by propeller sheet cavitation is closely related to the cavitation volume variation, and consideration of the cavity motion and the near-field effect is required for an accurate prediction.

The governing equation can be derived by applying the acoustic method developed by Ffowcs Williams and Hawkings (1983). The pressure fluctuation due to a volume change in the sheet cavity is proportional to the mass acceleration effect, which is shown in Eq. (2).

$$p'(\vec{x},t)=\frac{1}{c_0{}^2}\frac{\partial^2 p'}{\partial t^2}-\nabla^2 p=\frac{1}{4\pi r}\frac{\partial}{\partial t}\left[\rho_0\dot{Q}(\tau^*)\right] \tag{2}$$

where p' is the pressure fluctuation, and ρ_0 and c_0 are the density and the speed of in the undisturbed medium. Q is the volume of the sheet cavitation, whose first and second derivatives are represented as $\dot{Q}$ and $\ddot{Q}$, respectively.

From the relation between the pressure fluctuation source term and the observation point, the following expression can be derived.

$$g(\tau^*)=\tau^*-t+\frac{c_0}{r}$$
$$r=c(t-\tau^*)=\left|\vec{x}-\vec{x}_s\right| \tag{3}$$

τ^* and t are the source and the observer time, and $\vec{x}$, $\vec{x}_s$ are the location of the observer and the source position.

The pressure fluctuation field, whose source strength is $q(\vec{x}_s,t)$, can be expressed as follows.

$$p'(\vec{x},t)=\int\frac{q(\vec{x}_s,\tau^*)}{4\pi|\vec{x}-\vec{x}_s|}d^3y \tag{4}$$

If the observation point is far away from the source while the cavitation is stationary, the solution can be obtained as shown in Eq. (1) and according to Green′s function theorem for the wave equation. However, because the sheet cavitation rotates with the blades as the volume changes, the source term in Eq. (2) can be expressed as shown in Eq. (5) by considering the relative velocity of the observer.

$$p'(\vec{x},t)=\frac{\partial}{\partial t}\left[\frac{\rho_0\dot{Q}(\tau^*)}{4\pi r(1-M_r)}\right] \tag{5}$$

Here, a few relational expressions will be introduced for the physical phenomena. The relative velocity (v_r) can be obtained by differentiating the distance from source time.

$$\frac{\partial r}{\partial\tau^*}=-v_r$$
$$M_r=\vec{v}\cdot\hat{r}/c_0=v_i\cdot\hat{r}_i/c_0$$
$$M_i=v_i/c_0 \tag{6}$$

Eq. (5) is then written as the following equation.

$$4\pi p'(\vec{x},t)=\frac{\rho_0\ddot{Q}(\tau^*)}{r(1-M_r)^2}+\frac{\rho_0\dot{Q}(\tau^*)\dot{M}_i\hat{r}_i}{r(1-M_r)^3}+\frac{\rho_0\dot{Q}(\tau^*)c_0(M_r-M^2)}{r^2(1-M^3{}_r)} \tag{7}$$

Eq. (7) represents the pressure fluctuation at the observer time t and position $\vec{x}$. The pressure fluctuation source radiates the pressure pulse at source time t and position $\vec{x}_s$. As the source is in

Table 3
Operating conditions of propellers.

	Case A	Case B	Case C
Propeller	Propeller A	Propeller B	Propeller C
Scale ratio	20.8	20.8	18.4
Ship speed	14.65 knot (7.54 m/s)	13.98 knot (7.18 m/s)	12.34 knot (6.34 m/s)
Full-scale propeller rpm	134.6	136.0	123.9
Advance coefficient	0.4338	0.3840	0.5395
Thrust coefficient	0.1705	0.1759	0.2254
Cavitation number, $\sigma_{n\ 0.7R}$	2.0765	2.0443	2.6729
Propeller tip clearance (m), t_c	1.686	1.630	1.251

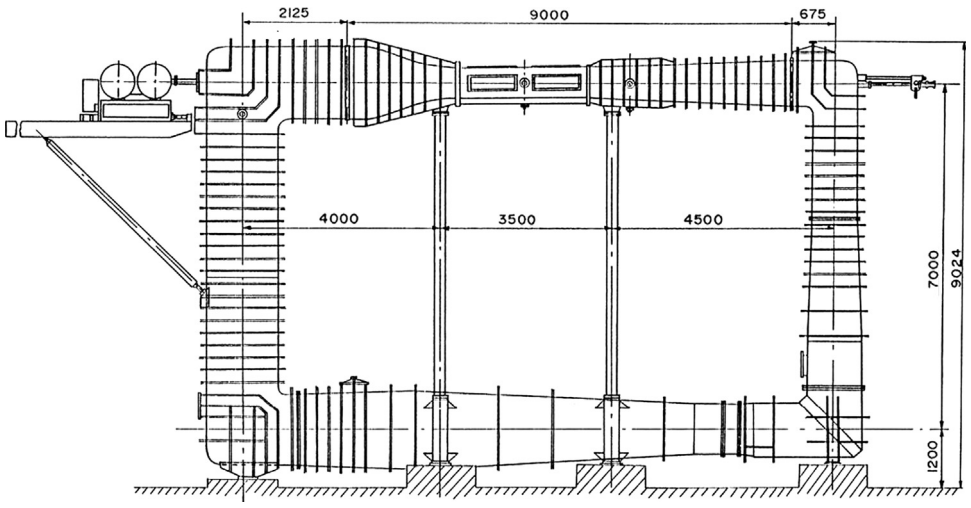

Fig. 7. Schematic diagram of the MOERI medium-sized cavitation tunnel.

motion, several terms affect the pressure fluctuation, as shown in Eq. (7). In each term, $(1-M_r)^{-1}$ is caused by the source movement. As the sheet cavitation moves with blades, the pressure fluctuation is stronger when the sheet cavity moves closer to the observer ($M_r > 0$) compared with when the sheet cavity move away from the observer ($M_r < 0$) even though the observation point is at the same distance from the source.

The first and second terms in Eq. (7) are the far-field terms, which are proportional to $1/r$, and the last term is the near-field term, which is proportional to $1/r^2$.

A numerical prediction tool has been developed based on Eq. (7). The sheet cavitation appears as a thin single volume of vapor attached to the blades near the leading edge and extending downstream. The sheet is obtained from a potential-based vortex lattice method. The time-dependent cavity volume variation results are used as the input for the developed numerical method to predict the pressure fluctuation.

The total volume of the cavity on the blade acts as a single volume of vapor. During the blade rotation, the varying inflow cause volume variation, and the radiated pressure pulse is caused by the acoustic monopole mechanism. The contributions from all the sheet cavities are summed. The retarded time equation is considered during the addition procedure. The retarded time is computed using a Newton iteration method. Contributions of each cavity, which each have a different retarded time, are added to form a pressure wave. The pressure history in the observer's time is then formed.

In this study, a flat horizontal plate is considered to simulate and predict the pressure fluctuation. According to Huse (1996),

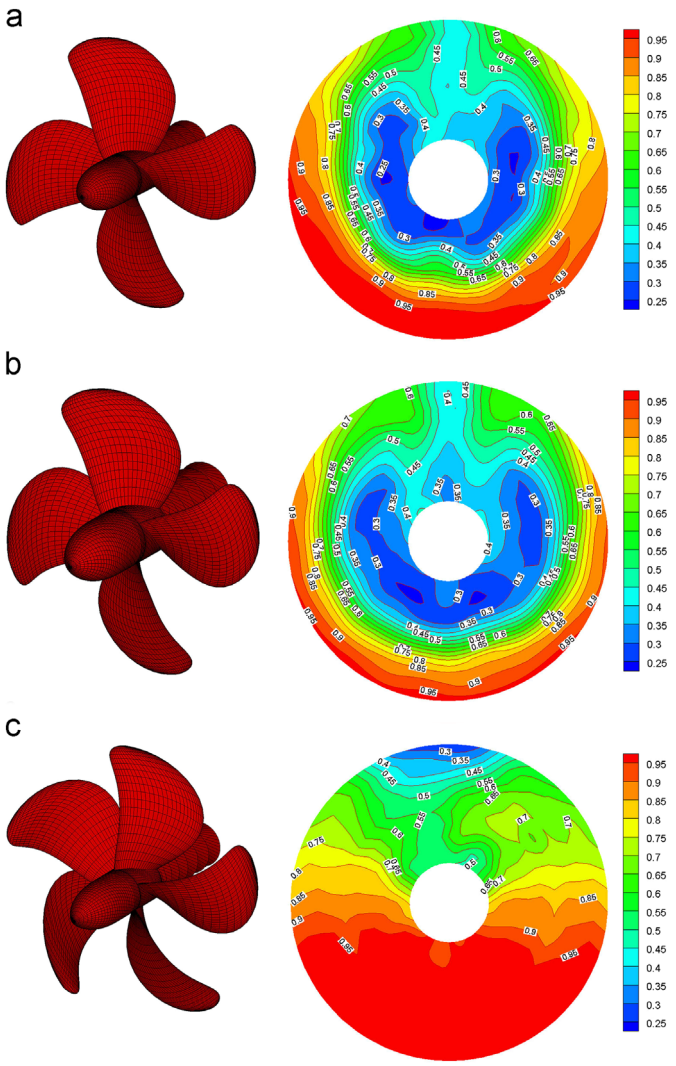

Fig. 8. Propeller configurations and nominal wake distributions; (a) propeller configuration and wake distribution for Case A (b) propeller configuration and wake distribution for Case B (c) propeller configuration and wake distribution for Case C.

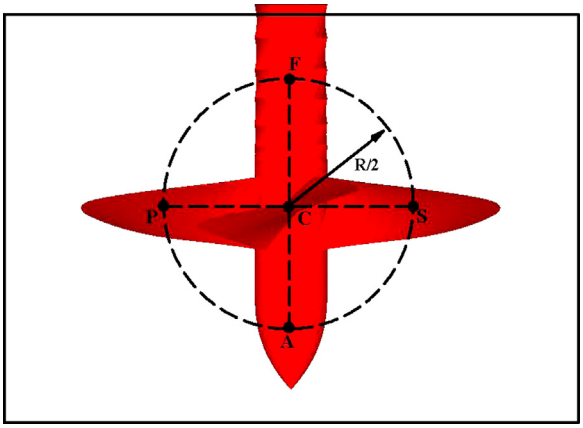

Fig. 9. Location of the five pressure transducers on the flat plate.

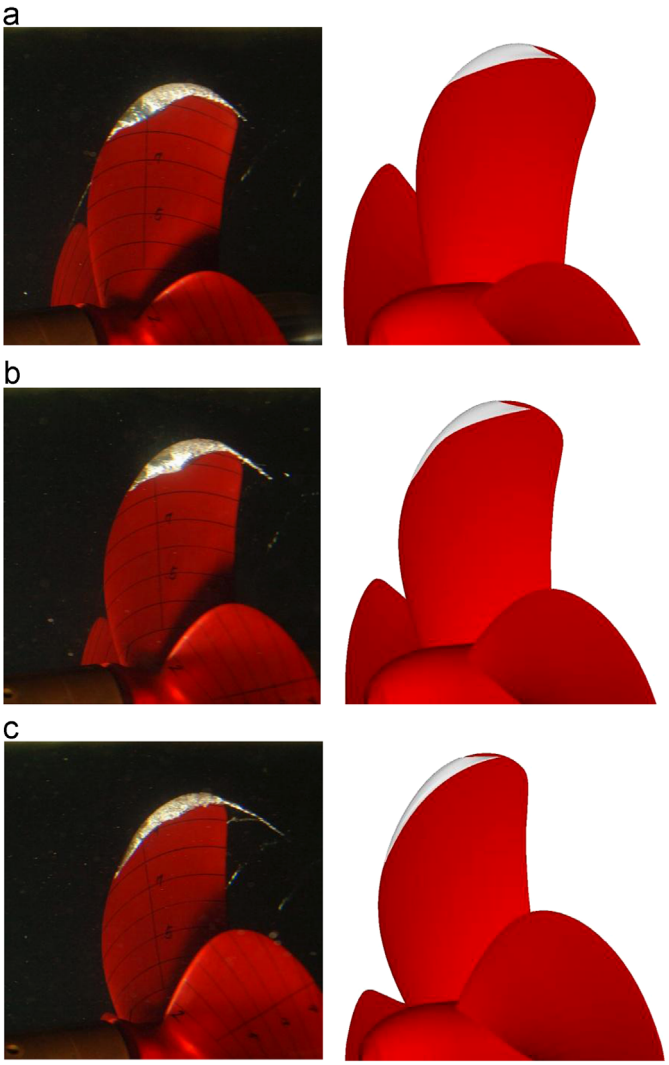

Fig. 10. Photographs of the cavitation patterns and results of the numerical flow solver (Case A) (a) Blade angle 0, (b) Blade angle 12, (c) Blade angle 18.

the solid boundary factor (SBF=2) is applied to the free field pressure computation results.

The time history of the pressure is transformed into the pressure fluctuation at the blade rate frequency using a Fourier transformation and a total pressure fluctuation is calculated by Eq. (8).

$$\tilde{P} = \sqrt{P_1{}^2 + 2P_2{}^2 + 3P_3{}^2 + 4P_4{}^2} \tag{8}$$

where, P_1: Pressure fluctuation at the first blade frequency, P_2: Pressure fluctuation at the second frequency, P_3: Pressure fluctuation at the third blade frequency, P_4: Pressure fluctuation at the fourth blade frequency.

2.2. Numerical simulations

The propeller sheet cavitation-induced pressure fluctuation is physically analyzed using the governing equation mentioned in the section above. The propeller model, the operating conditions, and the volume variation of the sheet cavitation are numerically assumed. Because various factors may affect the pressure fluctuation, these factors are simulated and analyzed.

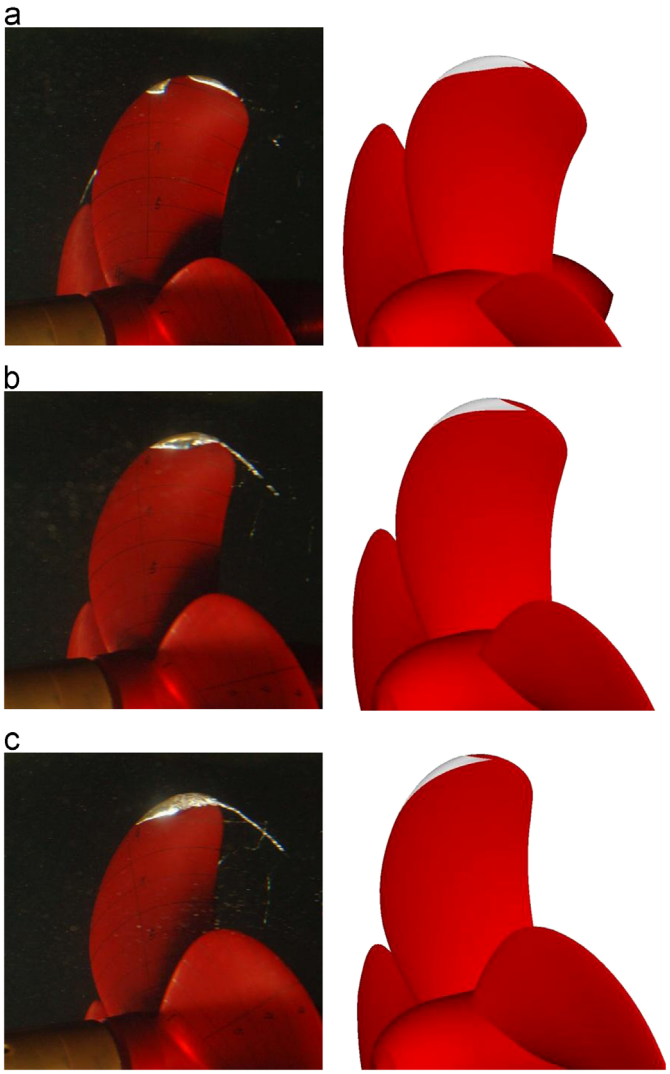

Fig. 11. Photographs of the cavitation patterns and results of the numerical flow solver (Case B) (a) Blade angle 0, (b) Blade angle 12, (c) Blade angle 18.

The numerically generated propeller configuration and the proposed propeller operating conditions are shown in Fig. 1 and Table 1, respectively. To analyze the effect of the source motion,

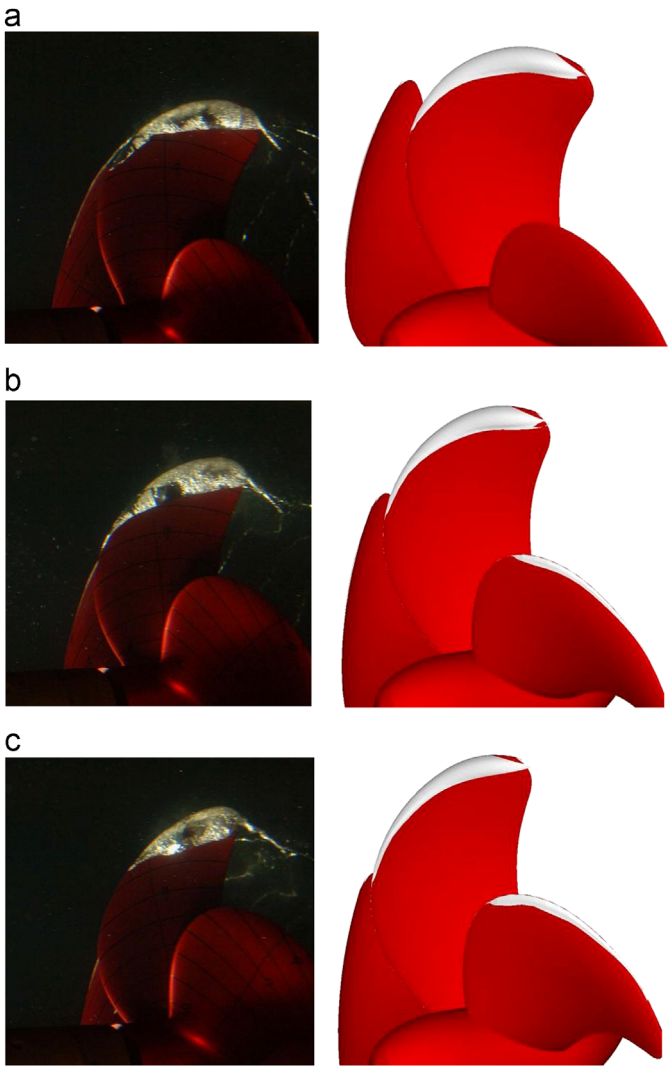

Fig. 12. Photographs of the cavitation patterns and the results of numerical flow solver (Case C) (a) Blade angle 0, (b) Blade angle 12, (c) Blade angle 18.

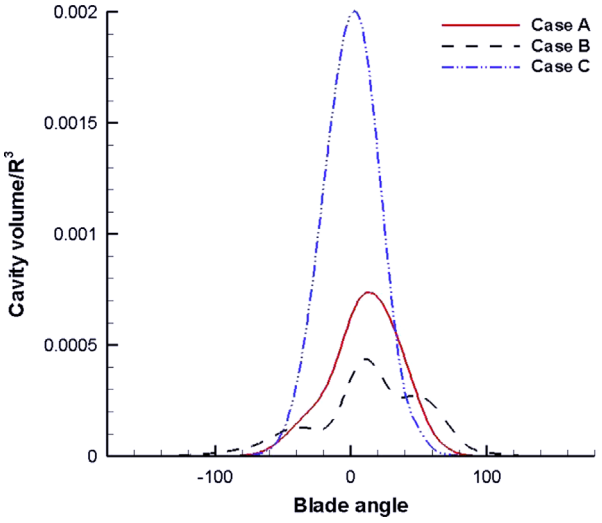

Fig. 13. Computed cavity volume variation using the vortex lattice method.

the symmetrical cavitation volume variation, whose maximum volume is located at blade angle 0, is assumed to be configured as shown in Fig. 2.

To find the formation mechanism of the pressure fluctuation, the pressure fluctuation induced by the sheet cavitation of each blade is calculated as shown in Fig. 3. This figure shows both the pressure fluctuation induced by the sheet cavity of each blade at point '*C*' of the rigid wall (above the propeller plane) and the resulting pressure fluctuation. Because the first blade moves from blade angle 0^o to blade angle 90^o and the fourth blade moves from -90^o to 0^o, these blades induce a relatively large pressure fluctuation. However, the second and third blades induce small pressure fluctuations because they produced little cavitation. Therefore, the resulting pressure fluctuation is represented by the summation of the pressure fluctuation induced by each blade, which all have phase differences.

The pressure fluctuation induced by sheet cavitation represents the summation of the near-field term and the far-field term. The extent to which each term affects the total pressure fluctuation is analyzed, as shown in Fig. 4. Fig. 4 shows the pressure fluctuation of the near-field and the far-field terms induced at point '*C*'.

To find the attenuation effect of each term according to the distance of the tip clearance, the near-field and the far-field terms are calculated at point '*C*' of the plate. The distance from the blade tip to the plate is assumed to be 0.5, 1.0, 3.0, 10.0, and 20.0 times the radius of the propeller. Fig. 5 shows the result of the computation. Because the near-field term is proportional to $1/r^2$ and the far-field term is to $1/r$, the near-field term is sharply reduced as it remains away from the source. Therefore, the far-field term is dominant at a distance. In general, the tip clearance between the hull and the propeller is less than 1.0, so the near-field term cannot be ignored, as shown in Fig. 5.

As specified above, if the relative velocity is not considered, the same pressure fluctuation values are expected at the same distance between the source and the observer point. However, if the relative velocity is considered, the results are somewhat different. Although the observer point is the same distance from the source, the induced pressure fluctuation results are stronger when the source becomes closer than when the source moves away from the observer. Therefore, the pressure fluctuation at position '*S*' is greater than the pressure fluctuation of position '*P*'. The maximum value of the pressure fluctuation is predicted to occur at a slightly starboard side of the propeller because the sources rotate to the right-hand side. These results are shown in Fig. 6.

3. Experimental validation

To validate the newly developed time domain prediction method, the results are compared with the experimental results and the results of potential-based numerical prediction methods for the various operating conditions and propellers.

The propeller cavitation flow results are obtained using a vortex lattice method developed by MOERI. The results of this method are used as the input for the numerical pressure fluctuation prediction methods, the potential-based prediction method (Kim et al., 1995), and the developed time domain prediction

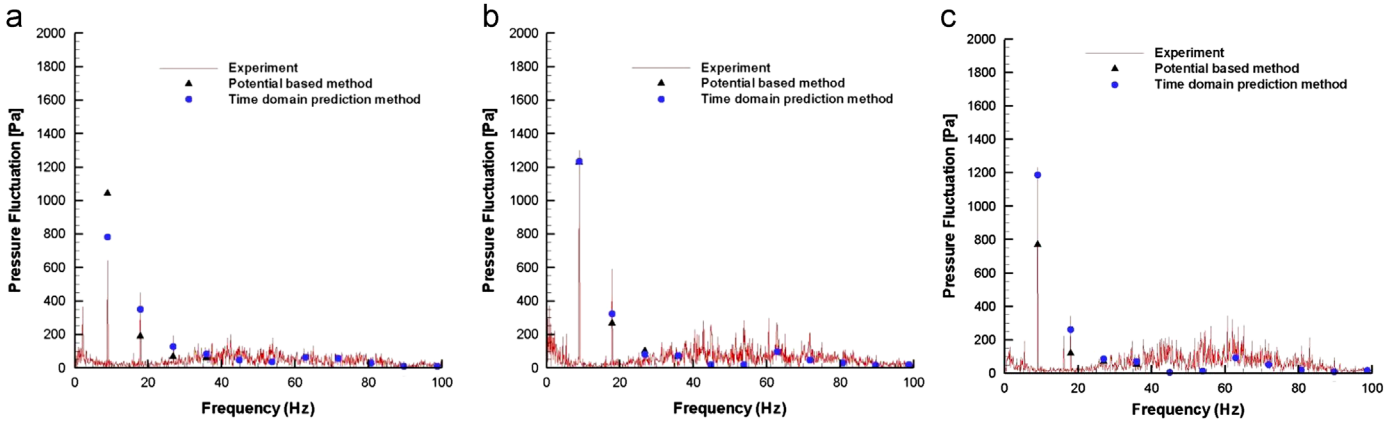

Fig. 14. Spectrum of the pressure fluctuation (Case A): (a) point '*P*'; (b) point '*C*'; and (c) point '*S*'.

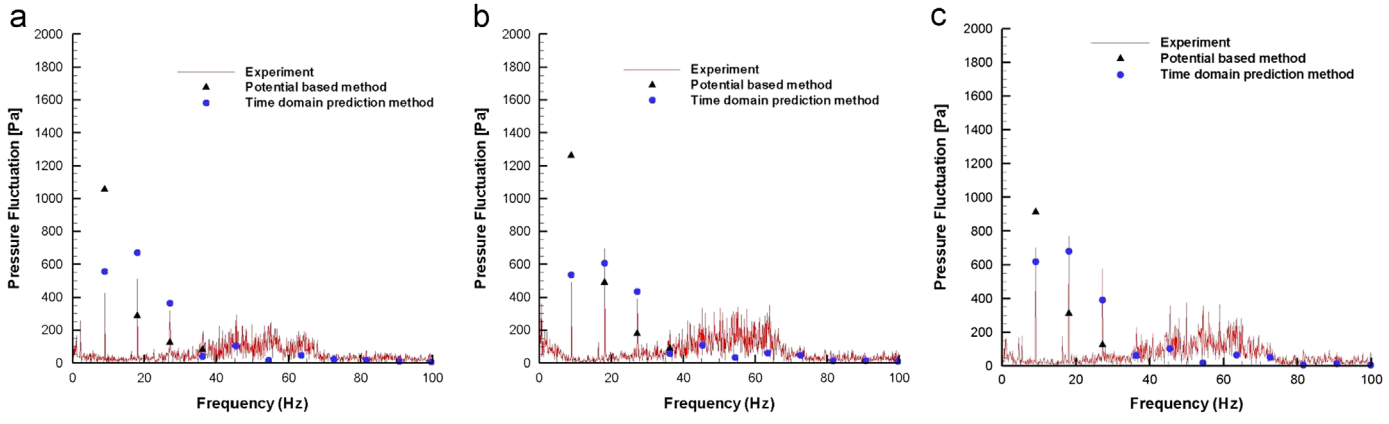

Fig. 15. Spectrum of the pressure fluctuation (Case B): (a) point '*P*'; (b) point '*C*'; and (c) point '*S*'.

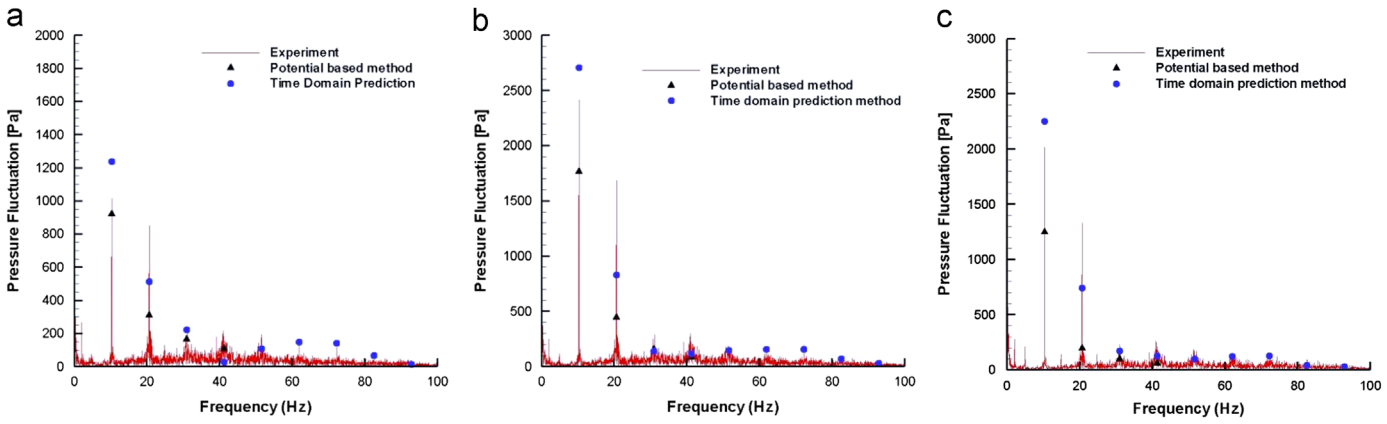

Fig. 16. Spectrum of the pressure fluctuation (Case C): (a) point '*P*'; (b) point '*C*'; and (c) point '*S*'.

Table 4
Total induced pressure fluctuation.

Total pressure fluctuation (Pa)	*P*	*C*	*S*
(a) Case A			
Experiment	995.6	1558.4	1333.6
Potential based method	1086.3	1297.9	803.0
Time domain prediction method	938.3	1329.3	1259.3
(b) Case B			
Experiment	1044.9	1355.6	1657.7
Potential based method	1157.3	1478.7	1040.9
Time domain prediction method	1263.2	1261.9	1336.3
(C) Case C			
Experiment	1580.5	3400.3	2816.8
Potential based method	1076.3	1898.4	1292.2
Time domain prediction method	1529.0	2966.1	2513.8

method. Details of the time domain prediction method are described in the section above.

A comparison between the computations and the experimental results can be made for the three cases shown in Table 2 and Table 3. These cases show the principal geometric parameters of the propellers and the operating conditions.

3.1. Experimental setup

A series of cavitation tests, including the cavitation observation and pressure fluctuation measurements, are carried out in the test section of the MOERI medium size cavitation tunnel. The test section of this tunnel is rectangular with a length of 2.6 m, a width of 0.6 m and a height of 0.6 m. The maximum flow speed is 12 m/s, and the pressure can vary from 10 to 200 kPa. A schematic diagram of the MOERI medium-sized tunnel is shown in Fig. 7.

A wake screen composed of a brass wire mesh was made to reproduce the nominal wake flow measured behind the model ship in the MOERI towing tank. The propeller configurations and the nominal wake distributions measured at the propeller plane inside the cavitation tunnel are shown in Fig. 8.

The pressure fluctuation is measured on a flat plate above the model propeller. The flat plate is away from the model propeller tip, which corresponds to the vertical clearance of the hull. Pressure transducers, model XTM-190-25A, were used to measure the pressure values. The computation and the five measured positions on the plate are shown in Fig. 9.

Using the method recommended by ITTC (1987), the full-scale pressure fluctuation amplitudes can be predicted from the model scale measurement according to the following formula.

$$P_S = P_M \times \frac{\rho_S}{\rho_M}\left(\frac{n_S}{n_M}\right)^2\left(\frac{D_S}{D_M}\right)^2$$

$$\frac{f_S}{f_M} = \frac{n_S}{n_M} \tag{9}$$

where ρ is the density, n is the rotational speed, and D is the diameter; suffix S represents the ship, and M represents the model.

3.2. Comparison results

The cavitation patterns of the model propellers are obtained for the selected blade's angular position, and the corresponding numerical flow analysis results are shown in Fig. 10, Fig. 11 and Fig. 12. The angular positions of a key blade shown in these figures are measured from the vertically upward position in a clockwise direction when the propeller is viewed from behind. Fig. 13 shows the computed sheet cavitation volume variations.

Fig. 14, Fig. 15 and Fig. 16 are the comparison results. The experimental result, the potential-based prediction results, and the results of the newly developed time domain prediction method are compared at positions '*P*', '*C*', and '*S*'.

As shown Table 4 and Fig. 17, the maximum value of the pressure fluctuation is experimentally measured and numerically predicted at a slightly starboard side of the propeller. There are two reasons. The first reason is that sheet cavitation volume is occurred analogously symmetric shape whose maximum volume is located slightly starboard side as shown in Fig. 13. The second reason is the source movement. Because sources are moving from port side to starboard side, induced pressure fluctuation at the starboard side is higher than that of port side.

The newly developed time domain prediction results show good agreement with the experimental results, and the developed method is qualitatively and quantitatively superior to the potential-based prediction method.

4. Conclusion

A new time domain prediction method has been presented with the aim of computing the pressure fluctuation induced by a propeller sheet cavitation. Modern acoustic theory is applied to the source modeling of the pressure fluctuation. Various factors affecting the pressure fluctuation are numerically simulated and analyzed based on the governing equation.

The pressure fluctuation induced by the propeller sheet cavitation is not simply proportional to the second derivative of the cavitation volume variation and inversely proportional to the

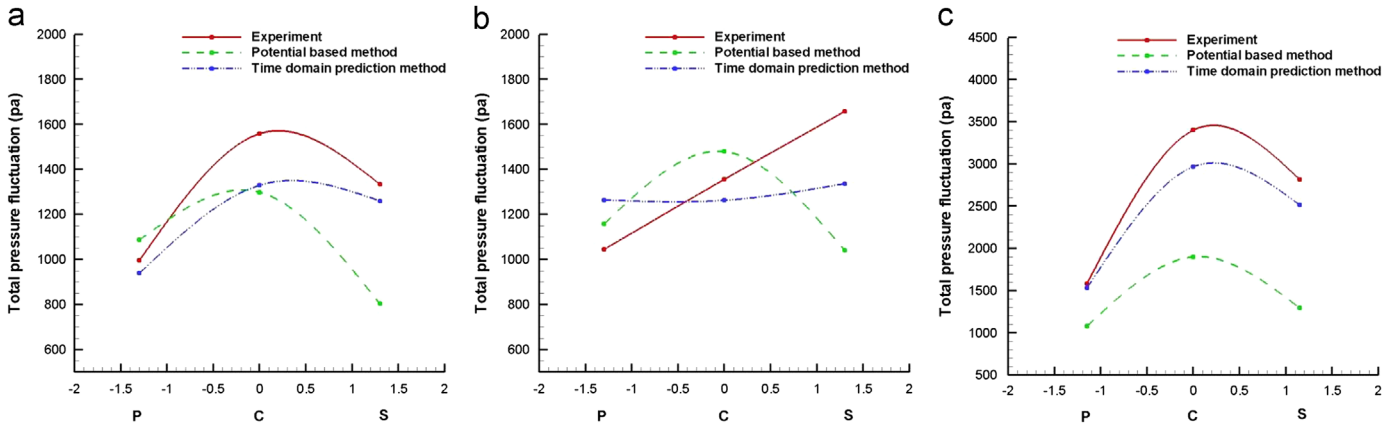

Fig. 17. Total induced pressure fluctuation: (a) Case A; (b) Case B; and (c) Case C.

distance between the source and the observer. As shown in Eq. (7), this pressure fluctuation is related to the first and second derivatives of the cavitation volume and is represented by the combined results of the far-field term and the near-field term. Various numerical simulations show that an elaborate prediction requires the overall consideration of the near-field effect, the source motion effect, and the retarded time.

The developed method has been evaluated using both the experimentally obtained results from a medium size cavitation tunnel test as well as the results form the potential-based prediction method for various propeller configurations and operating conditions. The numerically predicted flow and pressure fluctuation results are in agreement with the experimental results especially at the lower blade rate harmonics. The conclusion is that the presented numerical method results in a reasonable prediction of the pressure fluctuation due to propeller sheet cavitation.

The developed numerical prediction method and the findings will be useful sources for predicting the hull pressure fluctuation induced by a propeller at the design stage and for developing control technique. Moreover, these findings will be helpful in the field of propeller cavitation in the future.

Appendix: Nomenclature

c_0	speed of sound
$f(\vec{x},t)=0$	equation of the blade surface
l_i	local force per unit area of the fluid in direction i
M	Mach number
M_r	Mach number in the radiation direction
$\hat{n}$	unit outward normal vector to surface $f=0$
$p'(\vec{x},t)$	acoustic pressure
r	length of the radiation vector, $\lvert\vec{x}-\vec{y}\rvert$
$\vec{r}$	radiation vector, $\vec{x}-\vec{y}$
$\hat{r}$	unit radiation vector, $\vec{r}/r$
t	observer time
Q	cavitation volume
$\ddot{Q}$	acceleration of cavitation volume
R	cavitation radius
$\dot{R}$	cavitation radius wall velocity
$\ddot{R}$	cavitation radius wall acceleration
$\hat{t}$	unit tangent vector to the surface $f=0$
$\vec{v}$	local velocity of the blade surface
$\vec{x}$	observer position in the frame
$\vec{x}_{OBS}$	observer location
$\vec{y}$	source position
$\vec{y}_0(t)$	position vector from the origin of the ground-fixed frame to the moving frame
τ	source time
ret	evaluated at the retarded or the emission time

Acknowledgments

This work was supported by the Industrial Strategic Technology Development Program (10033668) funded by the Ministry of Knowledge Economy (MKE, Korea) and the Basic Research Program of MOERI/KIOST (PES156E).

References

Bark, G., 1988. On the Mechanisms of Propeller Cavitation Noise. Ph.D. Thesis. School of Mechanical Engineering, Charlmers University of Technology.
Blake, W.K., 1996. Mechanics of Flow-Induced Sound and Vibration. Orlando Academic Press Inc.
Carlton, J.S., 1994. Marine Propellers and Propulsion, second edition. Butterworth-Heinemann, Oxford.
Cavitation Committee Report, 1987. In: Proceedings of 15th International Towing Tank Conference, Hague.
Dowling, A.P., Ffowcs Williams, J.E., 1983. Sound and Sources of Sound. John Wiley & Sons.
Huse, E., 1996. Measurements of hull pressure fluctuation. In: Proceeding of the 21st International Towing Tank Conference, Trondheim, Norway.
Ji, B., Luo, X.W., Wang, X., Peng, X.X., Wu, Y.L., Xu, H.Y., 2011. Unsteady numerical simulation of cavitating turbulent flow around a highly skewed model marine propellerJ. Fluids Eng.-Trans. ASME 133 (1), 011102.
Ji, B., Luo, X.W., Peng, X.X., Wu, Y.L., Xu, H.Y., 2012. Numerical analysis of cavitation evolution and excited pressure fluctuation around a propeller in non-uniform wake. International Journal of Multiphase Flow 43, 13–21.
Kehr, Y.Z., Kao, J.H., 2011. Underwater acoustic field and pressure fluctuation on ship hull due to unsteady propeller sheet cavitation. Journal of Marine Science Technology 16 (3), 241–253.
Kerwin, J.E., Lee, C.-S, 1987. Prediction of Steady and Unsteady Marine Propeller Performance by Numerical Lifting-Surface Theory, Trans. SNAME Paper No. 8 Annual Meeting.
Kim, M.C., Kim, K.S., Song, I.H., 1996. A study of correlation between experiments and calculations of pressure fluctuation on hull surfaces. Journal of the Society of Naval Architectures Korea 33 (1), 19–26.
Kim, Y.G., Lee, C.S., Moon, I.S., 1995. Prediction of hull surface pressures induced by a cavitating propeller. In: Proceedings of Sixth International Symposium on Practical Design of Ships and Mobile Units, Seoul.
Kinnas, S.A., Fine, N.E., 1992. A nonlinear boundary element method for the analysis of unsteady propeller sheet cavitation. In: Proceedings of the 19th Symposium on Naval Hydrodynamic, Seoul.
Kinns, R., Bloor, C.D., 2004. Hull vibration excitation due to monopole and dipole propeller sources. Journal of Sound and Vibration 270, 951–980.
Lee, C.S., 1979. Prediction of Steady Unsteady Performance of Marine Propellers With of Without Cavitation by Numerical Lifting Surface Theory. Ph.D. Thesis. MIT, Department of Ocean Engineering.

Lee, C.S., Lee, J.T., Suh, J.C., Kim, Y.G., 1992. An analysis of excitation forces on the ship hull induced by the propeller. Journal of the Society of Naval Architectures Korea 29 (1), 81–92.

Luo, X.W., Ji, B., Peng, X.X., Xu, Hongyuan, Nishi, Michihiro, 2012. Numerical simulation of cavity shedding from a three dimensional twisted hydrofoil and induced pressure fluctuation by large-eddy simulation. Journal of Fluids Engineering 134 (4), 041202.

Merz, S., Kinns, R., Kessissoglou, N., 2009. Structural and acoustic responses of a submarine hull due to propeller forces. Journal of Sound Vibration 325, 266–286.

Pereira, F., Salvatore, F., Di Felice, F., 2004. Measurement and modeling of propeller cavitation in uniform inflowJournal of Fluids Engineering-Transactions ASME 126 (4), 671–679.

Seo, J.H., Moon, Y.J., Shin, B.R., 2008. Prediction of cavitating flow noise by direct numerical simulation. Journal of Computational Physics 227, 6511–6531.

The Specialist Committee on Cavitation Induced Pressures, 2002. In: Proceedings of 23rd International Towing Tank Conference, Venice, Italy.